Photodetection method using unbalanced sidebands for squeezed quantum noise in a gravitational wave interferometer

K. Somiya*
Department of Advanced Material Sciences, The University of Tokyo, Bunkyo-ku, Tokyo 113-0033, Japan
(Received 13 May 2002; revised manuscript received 3 December 2002; published 5 June 2003)

Homodyne detection is one of the ways to circumvent the standard quantum limit by changing the readout phase of a gravitational wave detector. In this paper it is shown that the readout phase can also be changed by the radio-frequency heterodyne detection scheme that is generally used in present detectors.

DOI: 10.1103/PhysRevD.67.122001 PACS number(s): 04.80.Nn, 42.50.Dv, 42.50.Lc, 95.55.Ym

I. INTRODUCTION

Several large-scale laser interferometric gravitational wave detectors have recently been developed. There are many kinds of noise sources that limit a detector's sensitivity, all of which, other than the quantum noise of the laser beams, may be reduced by technical advances in the near future. The laser beams used in these interferometers have coherent light which satisfies the least uncertainty relation between the number of photon and the phase of the light, which represents the particle and wave nature of light, respectively. Fluctuations in the photon number produce radiation-pressure noise on the test masses and fluctuations in phase produce shot noise. The shot noise can be reduced by increasing the laser power; however, this increases the radiation-pressure noise. Consequently there exists a sensitivity limit that is called the standard quantum limit (SQL) [1]. There are several ways to circumvent this SQL by unbalancing the coherent state, one of which is called homodyne detection [2]. In homodyne detection, the readout phase can be chosen by changing the homodyne phase ζ, reducing the quantum noise below the SQL. When ζ is chosen independently of the frequency, the SQL can be avoided only in a narrow band way, while a frequency dependent ζ, though very hard to obtain [3], could allow us to avoid the SQL in a broadband way. In this paper, we introduce a new detection method which is similar to the conventional scheme using an internal phase modulation to obtain the gravitational wave signal [4] and which does not require additional equipment other than the planned control system, but which can change the readout phase as easily as homodyne detection. In the broadband configuration which is currently used in gravitational wave detectors [5,6], the SQL cannot be avoided with this method because of an extra quantum noise [7–10], but this method is useful for the detuned configuration which will be employed in next generation detectors [11,12].

II. STANDARD QUANTUM LIMIT

Fluctuations in the photon number Δn and the phase of light $\Delta\phi$ are related to each other by Heisenberg's uncertainty principle. When the product of these two uncertainties is minimized, i.e., $\Delta n \cdot \Delta\phi = 1/2$, the light is said to be in a coherent state. In a laser beam the light is in a coherent state. The electric field of the laser beam is described by the following equation:

$$E_{\rm in} = \sqrt{N+\Delta n}\, e^{-i(\Omega t+\Delta\phi)} \simeq \left(1+\frac{\Delta n}{2N}+i\Delta\phi\right)\sqrt{N}e^{-i\Omega t}. \tag{1}$$

Here, N is the average photon number and Ω is the light frequency. From statistical theory, $\Delta n = \sqrt{N}$ so that $\Delta\phi = 1/2\sqrt{N}$. Thus the fluctuations of the real part and imaginary part of Eq. (1) are equal, a well-known property of the coherent state. Vacuum fluctuations of the electric field are independent of the photon number N; they can be injected in the detector from any transmissive optic such as the beam splitter or lossy mirrors [13,14].

Since the motion of the test mass induced by a gravitational wave of frequency ω produces a pair of sideband fields at frequencies $\Omega \pm \omega$, it is convenient to use the two-photon mode description introduced by Caves and Schumaker [15], in which a pair of photons are considered simultaneously. There are two combinations of the photon excitation quadratures written in terms of annihilation and creation operators (for details see Sec. II of Ref. [3]):

$$\hat{a}_1 = \frac{\hat{a}_+ + \hat{a}_-^\dagger}{\sqrt{2}}, \tag{2}$$

$$\hat{a}_2 = \frac{\hat{a}_+ - \hat{a}_-^\dagger}{\sqrt{2i}}. \tag{3}$$

Here, $\hat{a}$ and $\hat{a}^\dagger$ are the annihilation and creation operators, respectively, the suffix $\pm$ indicates the upper and lower operators whose frequencies are $\Omega+\omega$ and $\Omega-\omega$. Henceforth, we shall assume that the incident laser light is in the first quadrature. With this assumption $\hat{a}_1$ and $\hat{a}_2$ are the source of photon number and light phase vacuum fluctuations, respectively.

In an interferometer for gravitational wave detection the antisymmetric port of the beam splitter is kept dark (see Fig. 1) to maximize the signal compared to the shot noise; all the light but the gravitational wave signal is reflected to the symmetric port. These two ports are called the dark port and the bright port, respectively. Assuming perfect contrast for sim-

*Electronic address: somiya@hagi.t.u-tokyo.ac.jp

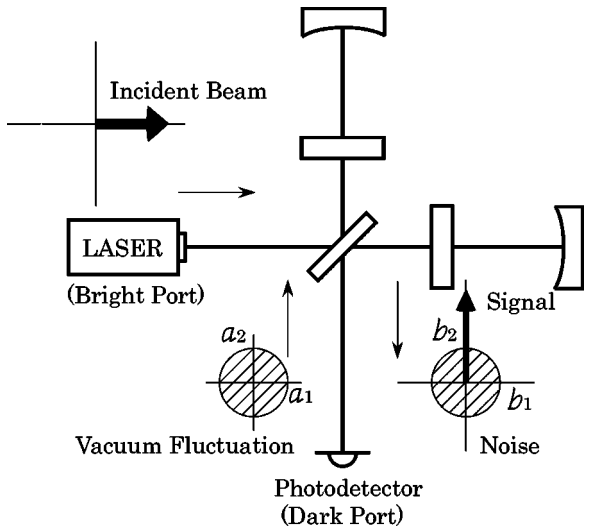

FIG. 1. The quantum noise of incident coherent light results from the vacuum fluctuation. The coordinate a_1 is the source of photon number fluctuation and a_2 is the source of phase fluctuation. Each of these coordinates consists of a pair of annihilation and creation operators.

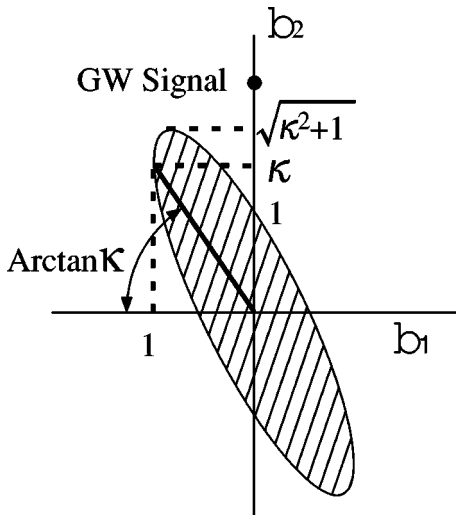

FIG. 2. The output quantum noise is squeezed by the effect of the radiation pressure. The quantum noise level is defined as the ratio between the differential signal and the projection of this ellipse to the b_2 axis.

plicity, there is no leakage carrier light at the dark port, which means a perfect-contrast interferometer. In this case the vacuum fluctuations coming from the direction of the laser are reflected to the bright port; only the vacuum fluctuation coming from the direction of the signal detection port can contribute quantum noise (Fig. 1). Furthermore we assume there is no optical loss in the interferometer; the end mirror reflectivities are unity.

The output field of the dark port consists of differential components including a gravitational wave signal and fluctuations in the light that are derived from a coupling between the incident beam and the vacuum fluctuations coming from the dark port. From the fact that the quadrature coordinates of the input field $\hat{a}_1$ and $\hat{a}_2$ are equal, one may think that the output field $\hat{b}_1$ and $\hat{b}_2$ are also balanced equally, but actually their amplitudes differ because of a coupling from photon number fluctuations to phase noise, known as radiation-pressure noise.

Following Ref. [3], we define $\kappa(\omega)$ as the coupling constant by which the radiation-pressure converts input $\hat{a}_1$ into output $\hat{b}_2$,

$$\begin{pmatrix} \hat{b}_1 \\ \hat{b}_2 \end{pmatrix} = \begin{pmatrix} 1 & 0 \\ -\kappa(\omega) & 1 \end{pmatrix} \begin{pmatrix} \hat{a}_1 \\ \hat{a}_2 \end{pmatrix} e^{2i\lambda}, \tag{4}$$

$$\kappa(\omega) = \frac{(I_0/I_{\mathrm{SQL}})2\gamma^4}{\omega^2(\gamma^2+\omega^2)}. \tag{5}$$

Here we assume the interferometer configuration of TAMA [5] and initial Laser Interferometric Gravitational Wave Observatory (LIGO) [6] as an example. These interferometers are recombined Michelson interferometers with Fabry-Perot resonators in the arms. The phase shift 2λ is accumulated by the signal sideband during a round trip in the arm cavity, γ is the Fabry-Perot cavity pole frequency, I_0 is the light power at the beam splitter, and $I_{\mathrm{SQL}}=mL^2\gamma^4/4\Omega$ is the light power necessary to reach the SQL sensitivity at $\omega=\gamma$, when m is the mass of the mirror and L is the arm cavity length.

As a result, the quantum output field is depicted by a squeezed ellipse as shown in Fig. 2 with axes rotated by $(1/2)\mathrm{arccot}(\kappa/2)$. This effect is called ponderomotive squeezing and was first recognized by Braginsky and Manukin [16]. If conventional radio-frequency (rf) heterodyne detection is used as the readout scheme [4], the signal sideband, as well as the squeezed vacuum, combines with a local oscillator field or rf sideband of the light to produce a signal and noise at the photodetector, both of which are proportional to the amplitude of the local oscillator. The noise level is defined as the ratio between the projection of the quantum noise ellipse to the $\hat{b}_2$ axis and the signal appearing on that axis with the input noise level $\hat{a}_1$ and $\hat{a}_2$ scaled to unity, and the signal is proportional to the amplitude of the incident classical field $\sqrt{\kappa}$, so the sensitivity can be written

$$h_{\mathrm{n}} = h_{\mathrm{SQL}} \cdot \sqrt{\frac{\kappa^2+1}{2\kappa}}, \tag{6}$$

where $h_{\mathrm{SQL}} \equiv \sqrt{8\hbar/m\omega^2L^2}$ is the SQL sensitivity, which occurs when $\kappa=1$, or $I_0=I_{\mathrm{SQL}}$ and $\omega=\gamma$.

III. CONVENTIONAL DETECTION AND HOMODYNE DETECTION

Over the last few decades, several theoretical efforts to overcome the SQL have been made [2,17–19], so-called ''quantum nondemolition'' (QND) techniques [20]. One such scheme is homodyne detection [2] which allows the phase of the local oscillator to be adjusted relative to the signal and noise ellipse so that the readout can occur for instance along

the minor axis of the noise ellipse, where the quantum noise is minimized, rather than simply along the $\hat{b}_1$ or $\hat{b}_2$ axis, like conventional detection.

In conventional detection we use rf sidebands for a modulation-demodulation scheme that produces the following field components at the photodetector:

$$\text{signal:} \quad 2iD\sin\psi(t),$$

$$\text{sidebands:} \quad -4i\alpha\cos\omega_{\rm m}t\sin\eta,$$

$$\text{vacuum:} \quad b_1\cos[\xi(t)+\phi_1]+b_2 i\sin[\xi(t)+\phi_2].$$

Here the common factor $e^{-i\Omega t}$ is omitted for simplicity (just as is shown in the phasor diagram). D is the classical amplitude of the carrier, $\psi(t)$ is the phase shift by gravitational waves, α is the amplitude of the sidebands, η is the phase shift caused by an asymmetry that is necessary to leak the sidebands to the dark port, $b_1=1$ and $b_2=\sqrt{\kappa^2+1}$ are the amplitudes of the common and the differential mode operators of the squeezed vacuum, ξ is an ellipse parameter which represents random noise, and the phase shifts ϕ_1 and ϕ_2 are given as follows:

$$\theta=\frac{1}{2}\text{arccot}\frac{\kappa}{2},$$

$$B_1^2=(\kappa\sin\theta-\cos\theta)^2+\sin\theta^2,$$

$$B_2^2=(\kappa\cos\theta-\sin\theta)^2+\cos\theta^2,$$

$$\phi_1=\arctan[B_2\sin\theta/B_1\cos\theta], \tag{7}$$

$$\phi_2=\arctan[B_1\sin\theta/B_2\cos\theta]. \tag{8}$$

The signal, sidebands, and vacuum components shown above are summed and squared by the photodetector:

$$\begin{aligned}&|\text{signal}+\text{sidebands}+\text{vacuum}|^2\\&=4b_2D\sin\psi(t)\sin[\xi(t)+\phi_2]+b_1^2\cos^2[\xi(t)+\phi_1]\\&\quad-16D\alpha\sin\psi(t)\underline{\cos\omega_{\rm m}t}\sin\eta+b_2^2\sin^2[\xi(t)+\phi_2]\\&\quad-8\alpha b_2\underline{\cos\omega_{\rm m}t}\sin[\xi(t)+\phi_2]\sin\eta+4D^2\sin^2\psi(t)\\&\quad+16\alpha^2\cos^2\omega_{\rm m}t\sin^2\eta.\end{aligned} \tag{9}$$

Multiplying the signal by $\cos\omega_{\rm m}t$ to extract the amplitude of the underlined components at $\omega_{\rm m}$, a process called demodulation, we obtain the signal-to-noise ratio as follows. The random noise parameter $\xi(t)$ is time-averaged:

$$\begin{aligned}[\text{demodulated signal}+\text{noise}]=&-8\alpha\frac{\sqrt{\kappa}}{2}\frac{h}{h_{\rm SQL}}\\&-2\sqrt{2}\alpha\sqrt{\kappa^2+1}.\end{aligned} \tag{10}$$

Here we define the signal produced by a strain h as

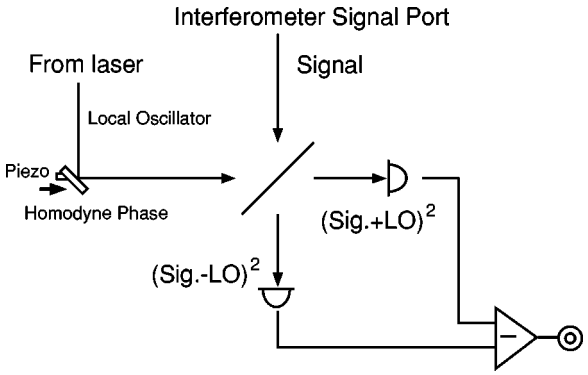

FIG. 3. One example to realize homodyne detection. The light with carrier frequency is picked off from the laser to be used as a local oscillator for the signal detection of the interferometer.

$$D\sin\psi(t)=\frac{\sqrt{\kappa}}{2}\frac{h}{h_{\rm SQL}}. \tag{11}$$

And then the noise spectral density reads

$$S_h=h_n^2=\frac{h_{\rm SQL}^2}{2}\left(\kappa+\frac{1}{\kappa}\right)\geqslant h_{\rm SQL}^2, \tag{12}$$

which indicates that we cannot overcome the SQL with conventional detection.

In homodyne detection, the local oscillators are combined with the signal light both with and without a π phase shift as is shown in Fig. 3. This can be realized by placing a beam splitter at the signal extraction port and injecting the incident light and the signal from opposite sides of the beam splitter. The squeezed vacuum injected from the output beam splitter is canceled by this process and the local oscillator can be considered as a classical light:

$$\text{LO:} \quad \beta\cos\zeta+\beta i\sin\zeta,$$

where β is the amplitude of the local oscillator and ζ is a readout phase called the homodyne phase, i.e., the phase of the local oscillator relative to the phase of the carrier light. Subtraction of the two interfered beams after square-law detection gives the following equation:

$$\begin{aligned}&\frac{1}{2}\{|\text{vacuum}+\text{signal}+\text{LO}|^2-|\text{vacuum}+\text{signal}-\text{LO}|^2\}\\&=2\beta\sin\zeta\left[\sqrt{\frac{1+(\kappa-\cot\zeta)^2}{2}}+2D\sin\psi(t)\right],\end{aligned} \tag{13}$$

and the noise spectral density reads

$$S_h=\frac{h_{\rm SQL}^2}{2}\frac{1+(\kappa-\cot\zeta)^2}{\kappa}, \tag{14}$$

which has a minimum value when the homodyne phase is $\zeta=\text{arccot}\,\kappa$. This result has been derived in previous papers [2,3]. We can see that the radiation-pressure effect disappears at a particular frequency (Fig. 4).

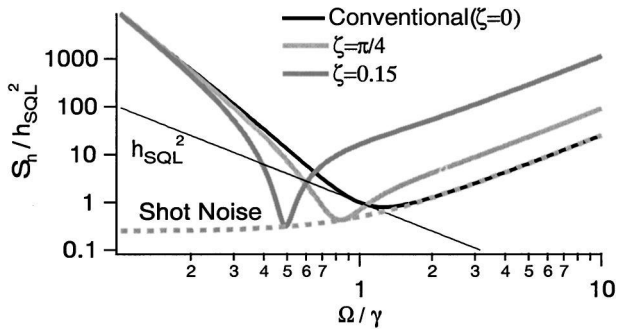

FIG. 4. Using homodyne detection, it is possible to overcome the SQL for a limited frequency band. The center frequency can be changed by adjusting the homodyne phase. The minimum value of each spectrum is limited only by shot noise, i.e., quantum noise without radiation-pressure noise.

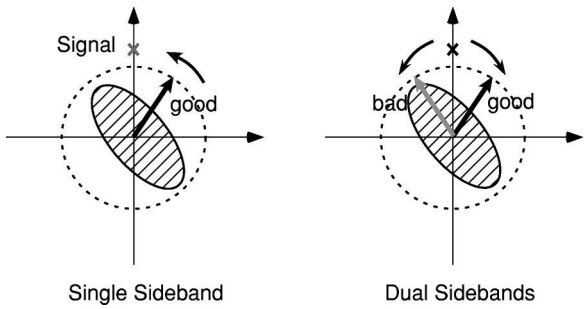

FIG. 5. Signal detection can be done at any phase for single sideband detection, but for conventional dual sidebands detection the other sideband will produce a worse signal-to-noise ratio.

IV. UNBALANCED SIDEBAND DETECTION

In this section we show that a performance identical to that achieved by homodyne detection can be achieved by using only a single sideband—without any additional optics such as the output beam splitter. The following analysis neglects what is called nonstationary shot noise, which will be discussed in Sec. VI A:

$$\text{single sideband:} \quad -2i\alpha e^{i\omega_m t}\sin\eta.$$

The solution to Eq. (9) with only a single sideband is as follows:

$$\begin{aligned}
&|\text{signal}+\text{single sideband}+\text{vacuum}|^2 \\
&\quad = 4b_2 D\sin\psi(t)\sin[\xi(t)+\phi_2]+4D^2\sin^2\psi(t) \\
&\quad\quad -4\alpha b_2 \underline{\cos\omega_m t}\sin[\xi(t)+\phi_2]\sin\eta \\
&\quad\quad -8\alpha D\sin\psi(t)\underline{\cos\omega_m t}\sin\eta+4\alpha^2\sin^2\eta \\
&\quad\quad +b_1^2\cos^2[\xi(t)+\phi_1]+b_2^2\sin^2[\xi(t)+\phi_2] \\
&\quad\quad +4\alpha b_1 \underline{\sin\omega_m t}\cos(\xi(t)+\phi_1)\sin\eta. \qquad (15)
\end{aligned}$$

After applying the same demodulation process as done for the conventional detection scheme, i.e., multiplying by $\sin(\omega_m-\zeta')$, the output is

$$2\alpha\sin\zeta'\left[\sqrt{\frac{1+(\kappa-\cot\zeta')^2}{2}}+2D\sin\psi(t)\right], \qquad (16)$$

which is the same as Eq. (13) except $\alpha\to\beta$ and $\zeta\to\zeta'$. Notice that the readout phase ζ' is not a homodyne phase but a heterodyne demodulation phase, i.e., the phase shift between the modulation sidebands and the rf demodulation signal. Conventionally, to obtain a differential signal, the demodulation phase is set to be $\pi/2$, but considering the ponderomotive squeezing effect, in order to minimize the quantum noise at the desired observing frequency band, the phase should be set to $\zeta'=\text{arccot}\,\kappa$.

One may wonder why this single sideband detection can avoid the SQL even though it is impossible with conventional dual sidebands detection. Figure 5 explains the reason clearly. With conventional detection using dual sidebands, even if one wants to optimize the demodulation phase for one sideband, the other sideband phase is antioptimal and generates increased noise. As a result the total noise is equivalent to the case when the sidebands stay on the differential axis.

This detection can also be realized with dual sidebands if there is an unbalance between the amplitude of the upper and lower sidebands. It can be derived that the noise spectrum in that case is the same as Eq. (14) when the demodulation phase meets the following condition:

$$\zeta'=\text{arccot}\frac{\alpha}{\Delta\alpha}\kappa. \qquad (17)$$

Here, α and $\Delta\alpha$ are the average and the difference of the amplitude of the upper and the lower sidebands. When the unbalance factor $\Delta\alpha$ is small, the output (16) is small, although the signal-to-noise ratio is unaffected.

There are several ways to produce an unbalance of the sidebands, for example, one can make only one sideband resonate in a cavity placed at the dark port. Advanced-LIGO will employ what is called a detuned resonant-sideband-extraction (RSE) system, realized with a signal recycling cavity detuned from the resonant condition (Fig. 6). To control the detuned cavity, it is planned to make only the upper or lower sideband resonant, hence, the carrier is detuned from resonance [11,12]. The transmittance of the RSE cavity for the resonant sideband is larger than the non-resonant sideband, producing the necessary sideband unbalance.

V. DETUNED CONFIGURATION

With a signal recycling mirror at the dark port, the gravitational wave signal sidebands circulate in the signal recycling cavity, which consists of the signal recycling mirror and the compound mirror with phase shift $e^{\pm 2i\lambda}$. The transmitted signal through this cavity is

$$Y_\pm \propto De^{i\omega t}\times e^{i\phi}\times e^{\pm 2i\lambda}\frac{\tau}{1-\rho e^{2i(\phi\pm\lambda)}}. \qquad (18)$$

Here $\phi=\omega l_s/c$ is the detuning phase, and τ and ρ are the transmittance and reflectance of the RSE mirror. From Eq.

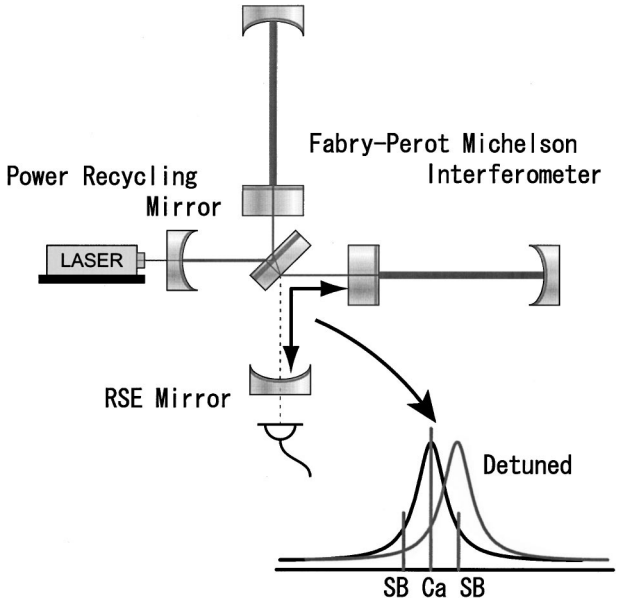

FIG. 6. Detuned RSE is realized by single-sideband locking which yields an unbalanced sideband condition.

(18) we can see that the amplitude of the upper and lower sideband is different, that is the total signal draws an ellipse on the phasor diagram.

The phase shift is different between the upper and lower sidebands:

$$\tan \psi_{\pm} = \frac{\rho \sin 2(\phi \pm \lambda)}{1 - \rho \cos 2(\phi \pm \lambda)}, \tag{19}$$

$$\psi = \frac{\psi_{+} + \psi_{-}}{2}. \tag{20}$$

The ellipse is inclined at an angle of $\phi + \psi$. While ϕ is fixed by the position of the RSE mirror, ψ varies with frequency. The output signal from a detector is given by the projection of the ellipse onto a direction that is determined by the readout phase.

When the laser power is sufficiently high, the reinjection of the signal induces radiation-pressure that enhances the signal at another frequency. This phenomenon is called the optical spring. In this case the noise spectrum due to the readout phase needs more complicated calculations, which were worked out in Refs. [17,21,22]. The result of the calculation is shown in Fig. 7 with several readout phases. The standard quantum limit is overcome by the effect of the optical spring and the shape of the spectrum changes with the different readout phases. Note that in the detuned configuration the quantum noise can no longer be simply identified as the shot noise and the radiation-pressure noise because these two components are strongly coupled.

VI. COMPARISON OF HOMODYNE AND UNBALANCED SIDEBAND DETECTION

The most interesting feature of unbalanced sideband detection is that no other equipment is required to change the readout phase. However, as we shall discuss in the next section, the unbalanced sideband detection has advantages and disadvantages compared with homodyne detection.

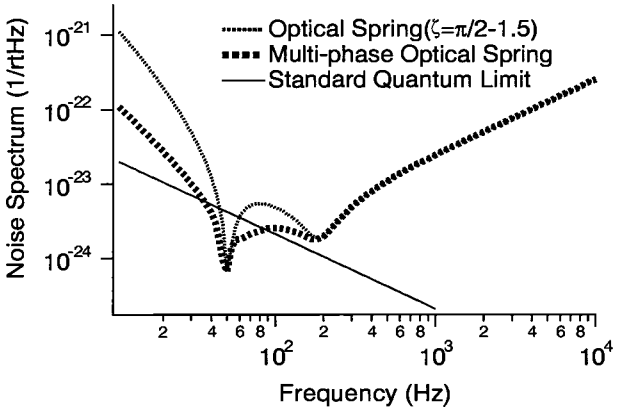

FIG. 7. The optical spring changes the shape of the noise spectrum with the readout phase. The laser power is 500 W, the finesse of the arm cavities is about 2000, the reflectivity of the RSE mirror is 0.98, and the detuning phase is 0.03° from the RSE condition. The homodyne phase or the demodulation phase for the thin solid line and the small dotted line is set to $\pi/2$ and $\pi/2-1.2$, respectively, and that for the large dotted line is chosen from $\pi/2$, $\pi/2-1.2$, and $\pi/2-1.5$ to be optimized at each frequency; this can be called a ''multi-phase optical spring.''

A. Nonstationary shot noise

An undesirable aspect of the unbalanced sideband detection is the influence of nonstationary shot noise, which is the shot noise generated during the demodulation process [7–9]. A vacuum fluctuation exists not only around the carrier frequency but also around the $\pm 2 f_{\mathrm{m}}$ region. Both incoherent noises are coupled to rf sidebands and square-summed when being demodulated by f_{m}. While the vacuum around the carrier is ponderomotively squeezed the vacuum around $\pm 2 f_{\mathrm{m}}$ is not squeezed so that the quadrature noise still remains for any demodulation phases (Fig. 8). If the readout phase is chosen far from $\pi/2$, the ratio from the signal to the original quantum noise may decrease while the ratio from the signal to the nonstationary shot noise increases and becomes dominant instead of the radiation-pressure noise at lower frequencies. As is discussed in Ref. [10], it is very hard to avoid the SQL in a broadband way with the unbalanced sideband

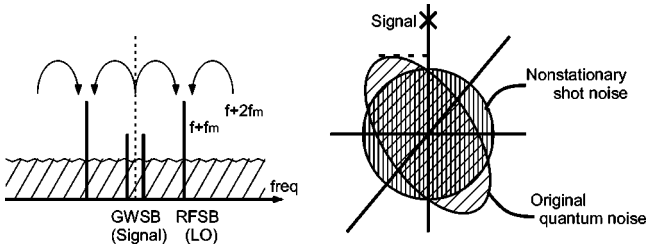

FIG. 8. A vacuum fluctuation from the $\pm 2 f_{\mathrm{m}}$ region generates the nonstationary shot noise during the demodulation process. If the readout phase is changed largely from $\pi/2$ the amount of the nonstationary shot noise exceeds that of the original quantum noise.

detection. For the detuned configuration, the readout phase should be optimized for the signal phase at the peak frequency to realize the best sensitivity; in this case the SQL can be avoided even with the effect of the nonstationary shot noise.

B. Multiphase detection

One advantage of unbalanced sideband detection is that one can combine the spectra of different demodulation phases. On the phasor diagram the single sideband rotates by its modulation frequency, for example, 12 MHz megahertz in initial-LIGO. Here the demodulation is a kind of the stroboscopic measurement [20], clipping the moving signal-to-noise ratio at some periodic phase and producing a spectrum for that phase. There is no quantum demolition if the measured *photocurrent* is split to several demodulator circuits, each of which has a different demodulation phase. There is, on the other hand, quantum demolition if the output *beam* is split to several photodetectors, because another vacuum fluctuation would be injected from the optical components used for the pick-off. In other words, if several *optical* local oscillators with different homodyne phases were to be used to try to avoid the SQL at several frequency bands, the decrease in optical power would increase the shot noise level, but if different-phase *electrical* local oscillators are used there is no corresponding increase in shot noise. By this technique we can obtain the thick dotted curve indicated in Fig. 7. (If we were able to remove the nonstationary shot noise in the conventional interferometer, the combined multiphase spectrum would be the dotted curve indicated in Fig. 4.)

VII. CONCLUSIONS AND DISCUSSIONS

In this paper, we introduce the rf unbalanced sideband detection as a photodetection method useful for future gravitational wave detectors. The unbalanced sideband detection can also change the readout phase and can help improve the sensitivity of the gravitational wave detector. The advantage of this method is that no additional equipment is required other than the planned control system for a future detector.

However, unlike homodyne detection, the rf detection introduces extra noise during the demodulation process [7–9]. While this nonstationary shot noise makes it hard to overcome the SQL for the broadband configuration, it is still possible to avoid the SQL through the effect of the optical spring when a detuned phase is used. The possibility of reducing the nonstationary shot noise by square wave modulation and demodulation, as suggested in Refs. [7–9], and squeezed input light could be investigated.

We also discuss the possibility of combining the spectrum from more than two ports with different readout phases, which could improve the sensitivity. This multiphase technique is available only for this unbalanced sideband detection, but cannot be achieved with homodyne detection.

A practical multiphase detection method for a high-power detuned RSE deserves more investigation. For example, the optical spring can generate instabilities between the arm cavities and the transmissive RSE mirror [21]. Such instabilities can be cured in the case of simple homodyne detection by damping the optical spring with a feedback control system [21]. The condition will be more complicated with a multiphase detection scheme, so further study is needed.

ACKNOWLEDGMENTS

The author wishes to thank Professor S. Kawamura, Professor N. Mio, and O. Miyakawa for giving the author a chance to think about this method. The author also wishes to thank members of Advanced-Interferometer-Configuration Committee from LSC (LIGO Science Collaboration) for many helpful comments, especially A. Buonanno and Y. Chen with whom important discussions were made privately. This research is supported by a Grant-in-Aid for Creative Basic Research of the Ministry of Education, Science, Sports and Culture.

[1] V.B. Braginsky, Sov. Phys. JETP **26**, 831 (1968).
[2] S.P. Vyatchanin and A.B. Matsko, JETP **82**, 1007 (1996).
[3] H.J. Kimble, Y. Levin, A.B. Matsko, K.S. Thorne, and S.P. Vyatchanin, Phys. Rev. D **65**, 022002 (2002).
[4] R. Weiss, Quarterly Progress Report, MIT Research Lab of Electronics **105**, 54 (1972).
[5] M. Ando *et al.*, Phys. Rev. Lett. **86**, 3950 (2001).
[6] D. Sigg, Class. Quantum Grav. **19**, 1429 (2002).
[7] T.M. Niebauer, R. Schilling, K. Danzmann, A. Rüdiger, and W. Winkler, Phys. Rev. A **43**, 5022 (1991).
[8] B.J. Meers and K.A. Strain, Phys. Rev. A **44**, 4693 (1991).
[9] N. Mio and K. Tsubono, Phys. Lett. A **164**, 255 (1992).
[10] A. Buonanno, Y. Chen, and N. Mavalvala, ''Quantum noise in laser-interferometer gravitational-wave detectors with a heterodyne readout scheme,'' gr-qc/0302041.
[11] AIC group report at LSC meeting 2001.
[12] J. Mason, Ph.D. thesis, California Institute of Technology, 2001.
[13] C.M. Caves, Phys. Rev. Lett. **45**, 75 (1980).
[14] C.M. Caves, Phys. Rev. D **23**, 1693 (1981).
[15] C.M. Caves and B.L. Schumaker, Phys. Rev. A **31**, 3068 (1985).
[16] V.B. Braginsky and A.B. Manukin, Zh. Éksp. Teor. Fiz. **52**, 987 (1967) [Sov. Phys. JETP **25**, 653 (1967)].
[17] A. Buonanno and Y. Chen, Phys. Rev. D **64**, 042006 (2001).
[18] W.G. Unruh, in *Quantum Optics, Experimental Gravitation, and Measurement Theory*, edited by P. Meystre and M.O. Scully (Plenum, New York, 1982), p. 647.
[19] V.B. Braginsky, M.L. Gorodetsky, F.Ya. Khalili, and K.S. Thorne, Phys. Rev. D **61**, 044002 (2000).
[20] V.B. Braginsky and F.Ya. Khalili, in *Quantum Measurement*, edited by K.S. Thorne (Cambridge University Press, Cambridge, England, 1992).
[21] A. Buonanno and Y. Chen, Phys. Rev. D **65**, 042001 (2002).
[22] A. Buonanno and Y. Chen, Phys. Rev. D **67**, 062002 (2003).